Advances in Consumer Research
https://acr-journal.com/

Volume-3 | Issue-1 | Jan 2026

Original Researcher Article

Luminescence Properties of Sm^{3+} Doped $Gd_2Si_2O_7$ Phosphors for Lighting Emitting Diodes

Nandanee Sahu[1]*, Rishi Jaiswal[1], Pradeep Dewangan[2]*
[1]Department of Physics, Shri Rawatpura Sarkar University, Raipur, Pin-492015, Chhattisgarh, India
[2]Department of Applied Physics, Shri Shankaracharya Institute of Professional Management and Technology, Raipur, Pin-492015, Chhattisgarh, India
***Corresponding author:**
Email ID: bnpithora@gmail.com, pradeep_dewangan15@rediffmail.com

Receive – 02 Dec 2025
Revised – 20 Dec 2025
Accepted – 15 Jan 2026
Publish – 30 Jan 2026

ABSTRACT
Solid-state lighting devices, thermoluminescence dosimeters, and photoluminescence dosimeters are commonly utilized in radiation environment monitoring. The development of new thermoluminescence and photoluminescence materials has become a primary focus in radiation dosimetry research, as the performance of dosimeters is directly tied to the materials used. As a result, the study and development of innovative thermoluminescence and photoluminescence materials have gained significant attention in recent years. In this study, the high-temperature solid-state method was employed to synthesize $Gd_2Si_2O_7$ doped with varying amounts of Sm^{3+}. To investigate the crystal structure, morphology, thermoluminescence (TL), and photoluminescence (PL) properties of Sm^{3+}-doped $Gd_2Si_2O_7$, a range of techniques, including X-ray diffraction (XRD), scanning electron microscopy (SEM), TL, and PL, were applied. The results revealed that the highest TL intensity occurred in $Gd_2Si_2O_7$ doped with 0.7 mol% Sm^{3+}, while the material also exhibited superior PL performance. Overall, $Gd_2Si_2O_7$ doped with 0.7 mol% Sm^{3+} shows significant promise for thermoluminescence dosimetry applications due to its outstanding TL properties. Additionally, the photoluminescence of the Sm^{3+}-doped $Gd_2Si_2O_7$ was analyzed.

1. INTRODUCTION:

Radiation dosimeters play a crucial role in ensuring environmental protection and public safety. Accurate dosimetry is vital not only for the effectiveness of radiation therapy in medicine but also for monitoring and managing radiation levels in the nuclear industry and environmental settings to protect both the public and workers from the risks associated with excessive radiation exposure [1–3]. As technological advancements continue, the demand for dosimeters with enhanced sensitivity and reliability has spurred increased research into new materials and methods for radiation detection [4]. Thermoluminescence (TL) and optically stimulated luminescence (OSL) technologies both depend on the ability of materials to absorb and store energy when exposed to radiation [5]. These materials subsequently release the stored energy as light when stimulated by heat or light, providing a detectable signal. TL technology is highly valued for its exceptional sensitivity to low radiation doses, while OSL is favored for its straightforward reading process and reusability [6]. The evolution of these technologies has expanded their application in various fields, including personal dose monitoring, environmental radiation surveillance, and medical dosimetry [7-8]. Phosphate compounds have shown significant potential in radiation dosimetry due to their superior luminescent properties and chemical stability [9]. These materials are particularly suited for TL and OSL dosimetry because of their excellent luminous characteristics [10]. Ongoing research aims to enhance their stability and luminous efficiency while also improving their responsiveness to different types of radiation. Recent advancements have led to considerable improvements in the luminescent properties of these materials, broadening their use in dosimetry applications [11–12].

Rare-earth-doped phosphate materials have become a major focus in radiation dosimeter research due to their unique electrical structures and luminous properties. The addition of rare-earth elements such as Thulium (Tm), Dysprosium (Dy), and Europium (Eu) significantly enhances the stability and luminous intensity of phosphate materials [13]. These doped materials exhibit improved thermoluminescence (TL) and optically stimulated luminescence (OSL) performance, including increased sensitivity, a broader linear response range, and enhanced environmental stability [14]. Consequently, rare-earth-doped phosphate materials are considered a promising direction for developing a new class of stable and effective radiation dosimeters [15–17]. Our recent study revealed that $Gd_2Si_2O_7$:Sm^{3+} samples synthesized using the sol-gel method exhibited higher thermal release intensity compared to those produced via the high-temperature solid-phase method. However, the optical release performance showed minimal variation between the two synthesis approaches [18]. In particular, $Gd_2Si_2O_7$ has gained attention as an ideal phosphate matrix due to its excellent luminous properties and strong chemical stability [19–23]. When doped with samarium (Sm), $Gd_2Si_2O_7$ demonstrates significant improvements in luminous performance, making it a promising candidate

in thermoluminescence dosimetry. $Gd_2Si_2O_7:Sm^{3+}$ has become a central topic in radiation dosimeter research, as Sm^{3+} doping not only enhances the luminous efficiency of $Gd_2Si_2O_7$ but also boosts its responsiveness to environmental radiation [24]. Given its superior thermoluminescence and photoluminescence properties, $Gd_2Si_2O_7:Sm^{3+}$ holds considerable potential for various applications in radiation dosimetry, including environmental radiation monitoring and medical dosimetry.

2. Materials and methods

2.1 High-temperature solid-state method

In this study, the high-temperature solid-state method was employed to synthesize $Gd_2Si_2O_7$ doped with various concentrations of Sm (0.1, 0.3, 0.5, 0.7, 0.9, 1.1, and 1.3 mol%). Stoichiometric amounts of the dopants Gd_2O_3 (A.R.), SiO_2 (A.R.), and Sm_2O_3 (A.R.) were carefully weighed and mixed, with the exception of those used in the preparation of undoped $Gd_2Si_2O_7$. The raw materials were thoroughly ground in an agate mortar and pestle for three hours. The resulting mixture was then placed in a crucible and sintered in a programmed muffle furnace at 700°C for two hours. After cooling to room temperature in a dust-free environment, the sample was ground again for two hours and sintered a second time at 1200°C for two hours. Following this, the sample was ground once more to obtain an ultrafine powder.

2.2 Methods of characterization

The crystal structure of the materials was characterized using the German BRUKER D8-ADVANCE X-ray diffractometer (XRD), which employed Cu Kα radiation (λ = 1.54 Å) at 40 kV and 40 mA. The scanning range was between 15° and 80°, with a scan rate of 5°/min. To analyze the morphology of $Gd_2Si_2O_7$ doped with 0.7 mol% Sm^{3+}, a HITACHI SU8010 Scanning electron microscope (SEM) was used. For optical measurements, the excitation and emission spectra of the samples were recorded using a RF-5301PC fluorescence spectrophotometer, with a 150W Xenon lamp and a slit width set to 5 nm. The scanning wavelength range was chosen between 200 and 900 nm, using white $Gd_2Si_2O_7:Sm^{3+}$ powder as the reference. The thermoluminescence (TL) light curves of the materials were captured with a Nucleonix TLD reader 1009I (manufactured by Hyderabad, India Pvt. Ltd.). The samples were exposed to 254 nm UV light for 15 minutes. TL measurements were conducted with a heating rate of 5°C/s, covering a temperature range from room temperature to approximately 300°C.

3. Results and discussion

3.1 XRD

Figure 1 displays the XRD patterns of $Gd_2Si_2O_7$ doped with various concentrations of Sm^{3+}, synthesized using the high-temperature solid-state method. The results confirm that the synthesized $Gd_2Si_2O_7:Sm^{3+}$ exhibits a single-phase orthorhombic structure with the space group Pnma. All peak values align with the Joint Committee on Powder Diffraction Standards (JCPDS) card number 96-152-6040, indicating that there are no additional crystal phases present in the samples and that $Gd_2Si_2O_7$ is the predominant crystalline phase. The XRD pattern, shown in Figure 1, also includes a local magnification for further clarity.

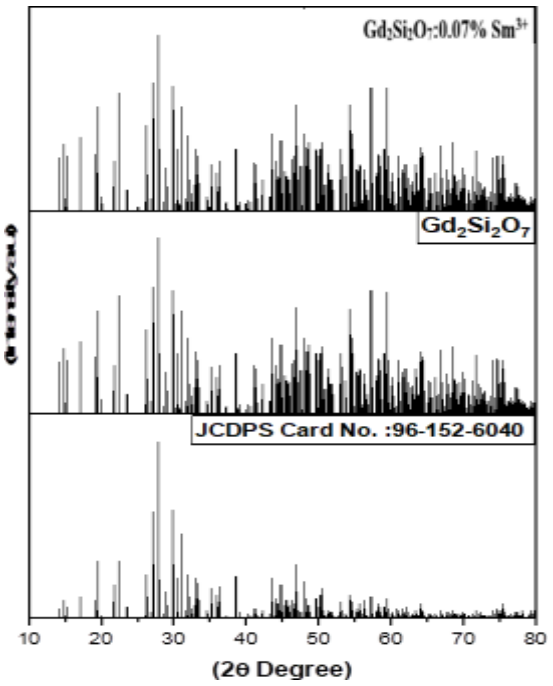

Figure 1: XRD Pattern of $Gd_2Si_2O_7:Sm^{3+}$

3.2 Surface morphology

Figure 2 presents the SEM images of $Gd_2Si_2O_7:Sm^{3+}$ (0.7 mol%) powder, revealing that the sample consists of irregularly shaped particles with some degree of agglomeration structure.

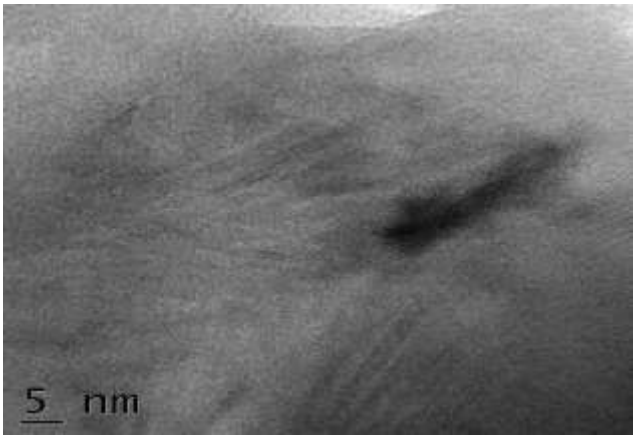

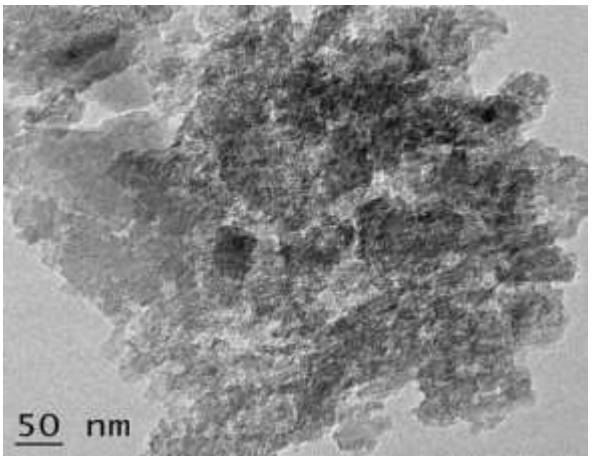

Figure 2: SEM image of $Gd_2Si_2O_7:Sm^{3+}$

3.4 Photoluminescence (PL)

The excitation spectra of $Gd_2Si_2O_7:Sm^{3+}$ phosphors with different concentrations of Sm^{3+} (0.1, 0.3, 0.5, 0.7, 0.9, 1.1 and 1.3 mol%) are shown in Fig. 3, which were measured at an emission wavelength of 603 nm. The plots show that in the 330 -560 nm, the observed eleven excitation peaks centered at 350, 360, 374, 402, 413, 423, 437, 459, 468, 471 and 480 nm correspond to the 4f-4f transitions from Sm^{3+}: $^6H_{5/2}$ to higher states, which are marked in Fig. 4. The most intense band at 402 nm is assigned to the Sm^{3+}: $^6H_{5/2} \rightarrow {}^4F_{7/2}$ transition, indicating that $Gd_2Si_2O_7:Sm^{3+}$ phosphors could be effectively pumped by 402 nm light [25-26]. Fig. 4 demonstrates the emission spectra of $Gd_2Si_2O_7:Sm^{3+}$ (0.1, 0.3, 0.5, 0.7, 0.9, 1.1 and 1.3 mol%) phosphors, which were excited by 402 nm. Four emissions peaks centered at 563, 603, 650 nm ascribed to transitions from Sm^{3+} ground state $^4G_{5/2}$ to $^6H_{5/2}$, $^6H_{7/2}$ and $^6H_{11/2}$ levels, respectively. Among them, the strongest emission peak located at 598 nm, which belongs to partially MD and partially forced ED transition. While the $^4G_{5/2} \rightarrow {}^6H_{9/2}$ is purely MD allowed transition and $^4G_{5/2} \rightarrow {}^6H_{9/2}$ is ED transition alone which is sensitive to crystal environment [27]. The intensity ratio of the ED (603 nm) to MD (563 nm) was calculated to reveal the symmetry of Sm^{3+} in the host environment. The results show that the ED/MD ratios are not varying much for different concentration of Sm^{3+}. Further, the emission intensity increases first and then decreases with Sm^{3+} concentration and reaches a maximum for x=0.07.

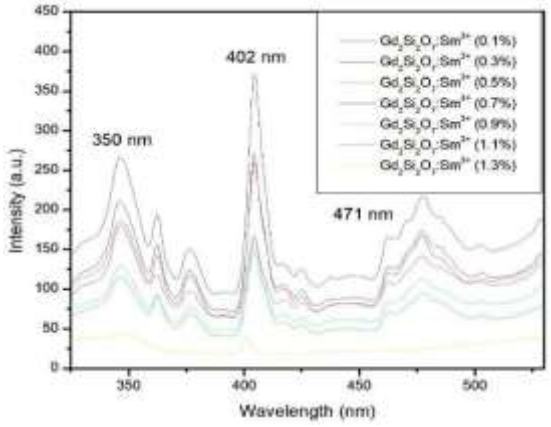

Figure 3: Excitation spectra of $Gd_2Si_2O_7:Sm^{3+}$ under 603 nm emission

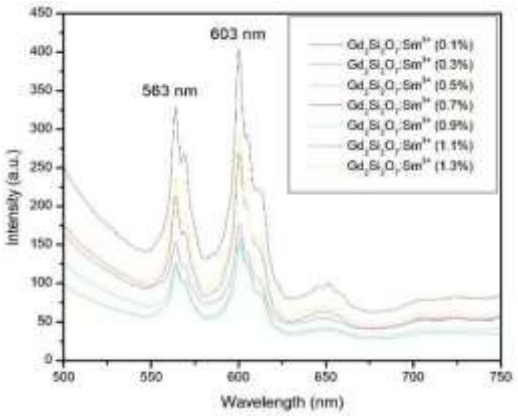

Figure 4: Emission spectra of $Gd_2Si_2O_7:Sm^{3+}$ under 402 excitations with different Dy^{3+} concentration

3.5 TL curves

Figure 5 presents the thermoluminescence glow curves of $Gd_2Si_2O_7:Sm^{3+}$ doped with varying concentrations of Sm^{3+}. In the 0 to 300 ℃ range, the sample displays luminescence peaks, with the most intense peak at 129.58 ℃. For $Gd_2Si_2O_7$doped with different concentrations of Sm^{3+} (0.1, 0.3, 0.5, 0.7, 0.9, 1.1 and 1.3 mol%), there is predominantly a single luminescence peak, which is also the strongest, located in the 0 to 300 ℃ range, at 129.58 ℃, respectively. Doping with Sm^{3+} alters the thermoluminescence intensity of $Gd_2Si_2O_7$ in the high-temperature region, with a general shift of the low-temperature peak positions towards the high-temperature region. The pyro release intensity in the high temperature area increased 2.4 times after Sm^{3+} doping. Figure 5 shows how the TL peak intensities of these samples vary with the dopant concentrations. It can be seen in the figure that the sample with dopant concentration of 0.5 mol% shows maximum TL peak intensity. The position, shape, and intensity of the thermoluminescence glow curve reflect the characteristics of the material's energy level traps [28]. Hence, by analyzing the thermoluminescence glow curve, various kinetic parameters can be estimated, including trap depth E, frequency factor s, kinetic order b, and release time t. A Gaussian fit was applied to the thermoluminescence glow curve of the 0.5 mol% Sm-doped sample, which shows the highest luminescence intensity among all samples, as shown in Figure 6 Using Chen's empirical formula in conjunction with the peak shape method, the kinetic parameters of the fitted curve were estimated by determining the peak temperature Tm, the half-maximum temperatures on the lower temperature side T_1, and on the higher temperature side T_2. The resulting kinetic parameters are presented. The frequency factor refers to the number of attempts per second made by trapped electrons to escape the trap, which, in conjunction with temperature and trap depth, determines the stability of the trap. The release time suggests a relatively long average lifetime for the trap. Smaller frequency factor values and the mean lifetime of larger traps indicate increased trap stability [29]. With a kinetic order b of 1.5, the thermoluminescence glow curve of the sample mainly follows a first-order kinetic equation.

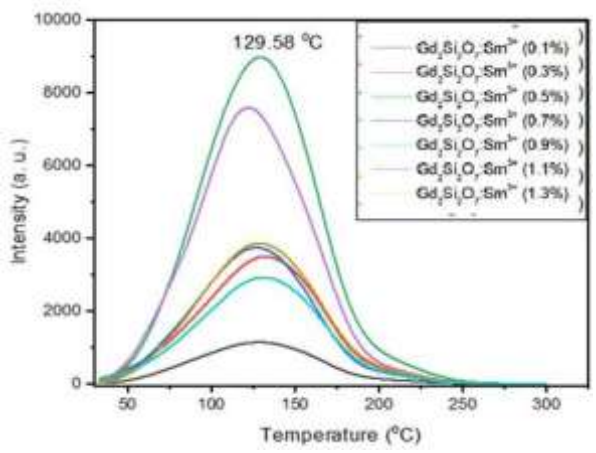

Figure 5: TL glow curve of $Gd_2Si_2O_7:Sm^{3+}$ with different Dy^{3+} concentration

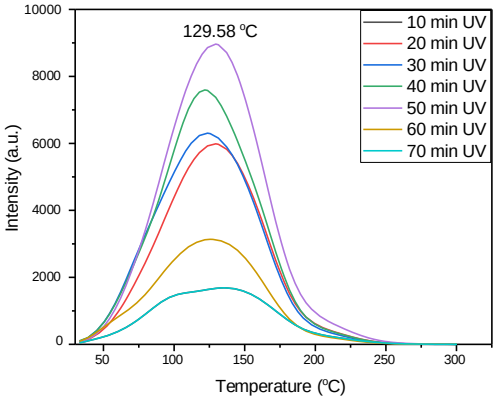

Figure 6: TL glow curve of $Gd_2Si_2O_7:Sm^{3+}$ with different UV exposure time

4. CONCLUSION

In this study, Sm^{3+} doped $Gd_2Si_2O_7$ phosphors were successfully synthesized using the high-temperature solid-state method, and their thermoluminescence (TL) behavior was systematically analyzed under varying dopant concentrations and UV irradiation durations. The TL intensity was found to be highly dependent on Sm^{3+} concentration, with an optimal performance at 0.7 mol%, beyond which concentration quenching effects were observed. Similarly, UV exposure time significantly influenced the TL response, with the maximum intensity obtained at 50 minutes, after which overexposure led to reduced emission due to trap saturation or recombination losses. The TL glow peak consistently appeared around 130°C across all conditions, indicating stable trapping centers. Kinetic parameters such as the glow peak temperature, full width at half maximum, and symmetry factor were evaluated, offering insight into the trap dynamics and glow curve characteristics. Although the calculated activation energy and frequency factor values were limited by assumptions in glow curve shape, the overall data support the conclusion that $Gd_2Si_2O_7:Sm^{3+}$ phosphor, particularly at 0.5 mol% doping and 50-minute UV exposure, is a promising candidate for TL-based radiation dosimetry. Its stable luminescence behavior, coupled with shallow trap levels, makes it suitable for reliable and repeatable dosimetric applications.

REFERENCES

[1] X. Chen, C. Jagadish and J. Ye, Oxide Electronics, pp. 235-352 (2021)

[2] J. Zhao, W. Zhang, E. Xie, Z. Ma, A. Zhao and Z. Liu, Appl. Surf. Sci. Vol. 257, pp. 4968-4972 (2011)

[3] Zh. Lu, L. Weng, Sh. Song, P. Zhang, X. Luo and X. Ren, Ceramics International, pp. 5305–5310 (2012)

[4] J. Xue, X. Wang, J. H. Jeong, and X. Yan, Physical Chemistry Chemical Physics, vol. 20, no. 17, pp. 11516-11541 (2018)

[5] S. Tripathi, R. Bose, A. Roy, S. Nair, and N. Ravishankar, ACS applied materials & interfaces, pp. 26430-26436 (2015)

[6] X. Huang and Q. Zhang, Journal of Applied Physics, pp. 053521 (2009)

[7] M. P. Saradhi and U. Varadaraju, Chemistry of materials, pp. 5267-5272 (2006)

[8] C. Zhu, J. Wang, M. Zhang, X. Ren, J. Shen, and Y. Yue., Journal of the American Ceramic Society, pp. 854-861. (2014)

[9] D. Golja and F. Dejene, Optik, pp. 1126-1132 (2019)

[10] Neha Lalotra, Manav Sharma, Kamni Pathania, Journal of Materials Science 59(27), 12630–12647, 2024.

[11] Shruti Dhale, N.S. Ugemuge, Vartika Singh, Manoj Singh Shekhawat, S.V. Moharil, Optical Materials, Volume 148, February 2024, Article 114888.

https://doi.org/10.1016/j.optmat.2023.114888

[12] C. C. (2024). Journal of Crystal Growth, 640, Article 127377.

[13] Khajuria, P., Mahajan, R., & Prakash, R. (2021). Journal of Materials Science: Materials in Electronics, 32, 27441–27448.

[14] Dhale, S. P., Ugemuge, N. S., Singh, V. S., & Moharil, S. V. (2025),Spectrochimica Acta Part A: Molecular and Biomolecular Spectroscopy, 325, 125050.

[15] Dhale, S. P., Ugemuge, N. S., Singh, V., & Moharil, S. V. (2024). Journal of Materials Science, 59(31), 16158–16169.

[16] D. Golja and F. Dejene, Journal of Alloys and Compounds, pp. 154216, 2020 (2020)

[17] A. Shukla, I. H. Jung, S. A. Decterov, and A. D. Pelton, Calphad, pp. 140-147 (2018)

[18] P. Dewangan, D. P. Bisen, N. Brahme and S. Sharma, Journal of Alloys and Compounds, 423-433 (2019)

[19] M. Goreaud, J. Choisnet, B. Raveau and A. Deschanvres, Revue de Chimie Minerale 207-216 (1974)

[20] Z. Zhou, A. Zhang, L. Zhou, Z. Hu, Y. Zhao, J. Chen, Y. Li, L. Zhao, B. Deng and R. Yu, J. Lumin. Vol. 251, pp. 119205 (2022)

[21] A. K. Singh, S. K. Singh and S. B. Rai, RSC Adv., 2014,4, 27039-27061.

[22] N. Hussain, S. Rubab and V. Kumar, Ceram. Int. Vol. 8 pp. 1-9 (2023)

[23] H. Ryu and H. D. Park, J. Ind. Eng. chem., pp. 177-181 (1997)

[24] J. T. Zhao, X. Y. Sun and Z. Q. Wang, Chem. Phys. Lett. Vol. 691, pp. 68-72 (2018).

[25] J. Sun, D. Ding, and J. sun, Optical Materials, 58, 188–195 (2016).

[26] G. Lu, K. Qiu, J. Li, W. Zhang, and X. Yuan, Luminescence, 32 93–99 (2017).

[27] C. Ji, Z. Huang, X. Tian, H. He, J. Wen, Y. Peng, J. Alloys Compd. 825 (2020) 154176, https://doi.org/10.1016/j. jallcom.2020.154176.

[28] B. Wang, Y. Liu, Z. Huang, and M. Fang, RSC Adv., 8, 15587-15594 (2018).

[29] P. Dewangan, D. P. Bisen, N. Brahme and S. Sharma, Jouranl of Alloys and Compounds, 777 (2019) 423-433.

..

.